70. Toyoizumi, T., Mick, R., Abbas, A. E., Kang, E. H., Kaiser, L. R., and Molnar-Kimber, K. L. (1999) Combined therapy with chemotherapeutic agents and herpes simplex virus type 1 ICP34.5 mutant (HSV-1716) in human non-small cell lung cancer. *Hum. Gene Ther.* **10,** 3013–3029.
71. Advani, S. J., Sibley, G. S., Song, P. Y., et al. (1998) Enhancement of replication of genetically engineered herpes simplex viruses by ionizing radiation: a new paradigm for destruction of therapeutically intractable tumors. *Gene Ther.* **5,** 160–165.
72. Bradley, J. D., Kataoka, Y., Advani, S., et al. (1999) Ionizing radiation improves survival in mice bearing intracranial high-grade gliomas injected with genetically modified herpes simplex virus. *Clin. Cancer Res.* **5,** 1517–1522.
73. Chung, S. M., Advani, S. J., Bradley, J. D., et al. (2002) The use of a genetically engineered herpes simplex virus (R7020) with ionizing radiation for experimental hepatoma. *Gene Ther.* **9,** 75–80.
74. Jorgensen, T. J., Katz, S., Wittmack, E. K., et al. (2001) Ionizing radiation does not alter the antitumor activity of herpes simplex virus vector G207 in subcutaneous tumor models of human and murine prostate cancer. *Neoplasia* **3,** 451–456.
75. Blank, S. V., Rubin, S. C., Coukos, G., Amin, K. M., Albelda, S. M., and Molnar-Kimber, K. L. (2002) Replication-selective herpes simplex virus type 1 mutant therapy of cervical cancer is enhanced by low-dose radiation. *Hum. Gene Ther.* **13,** 627–639.
76. Muldoon, L. L., Nilaver, G., Kroll, R. A., et al. (1995) Comparison of intracerebral inoculation and osmotic blood-brain barrier disruption for delivery of adenovirus, herpesvirus, and iron oxide particles to normal rat brain. *Am. J. Pathol.* **147,** 1840–1851.
77. Rainov, N. G., Zimmer, C., Chase, M., et al. (1995) Selective uptake of viral and monocrystalline particles delivered intra-arterially to experimental brain neoplasms. *Hum. Gene Ther.* **6,** 1543–1552.
78. Barnett, F. H., Rainov, N. G., Ikeda, K., et al. (1999) Selective delivery of herpes virus vectors to experimental brain tumors using RMP-7. *Cancer Gene Ther.* **6,** 14–20.
79. Ikeda, K., Ichikawa, T., Wakimoto, H., et al. (1999) Oncolytic virus therapy of multiple tumors in the brain requires suppression of innate and elicited antiviral responses. *Nat. Med.* **5,** 881–887.
80. Todo, T. (2002) Oncolytic virus therapy using genetically engineered herpes simplex viruses. *Hum. Cell* **15,** 151–159.
81. Spaete, R. R. and Frenkel, N. (1982) The herpes simplex virus amplicon: a new eukaryotic defective-virus cloning-amplifying vector. *Cell* **30,** 295–304.

Selective Expression of a Subset of Neuronal Genes in Oligodendroglioma with Chromosome 1p Loss

Akitake Mukasa[1, 2*]; Keisuke Ueki[4]; Xijin Ge[1]; Shumpei Ishikawa[1, 3]; Takafumi Ide[5]; Takamitsu Fujimaki[6]; Ryo Nishikawa[7]; Akio Asai[8]; Takaaki Kirino[2]; Hiroyuki Aburatani[1]

[1]Genome Science Division, Research Center for Advanced Science and Technology, [2]Department of Neurosurgery, [3]Department of Pathology, Graduate School of Medicine, University of Tokyo, Japan.
[4]Department of Neurosurgery, Dokkyo University School of Medicine, Japan.
[5]Department of Neurosurgery, Tokyo Metropolitan Bokuto Hospital, Japan.
[6]Department of Neurosurgery, School of Medicine, Teikyo University, Japan.
[7]Department of Neurosurgery, Saitama Medical School, Japan.
[8]Department of Neurosurgery, Saitama Medical Center/School, Japan.
*Current address: Ludwig Institute for Cancer Research, San Diego Branch, Calif.

Corresponding author:
Keisuke Ueki, MD, PhD, Department of Neurosurgery, Dokkyo University School of Medicine, 880 Kitakobayashi, Mibu, Tochigi 321-0293, Japan (E-mail: kuekitky@umin.ac.jp).

Gliomas are classified based mainly on microscopic resemblance to their presumed glial origin such as astrocyte and oligodendrocyte. However, more objective diagnostic criteria are indispensable for the precise treatment of patients. For instance, loss of the short arm of chromosome 1 (1p) in oligodendrogliomas is recognized as an important marker for better response to chemotherapy and longer survival of the patients. To gain insight into their molecular biological background and to identify genes characterizing each subgroup, we investigated gene expression profile of the 4 glioma subsets, oligodendroglioma with and without 1p loss, diffuse astrocytoma and glioblastoma using DNA microarray. Remarkably, most of the genes showing distinctive expression in oligodendroglioma with 1p loss were also highly expressed in normal brain tissues and had neuron-related function, which included *MYT1L, INA, RIMS2, SNAP91* and *SNCB*. Histological analysis also demonstrated that *MYT1L*, which were abundantly expressed in normal neuron, were certainly present in tumor cells. These results suggest that oligodendroglioma, especially with 1p loss, has more or less neuronal characteristics although oligodendroglioma is thought to originate form glial lineage cell. With further pathological studies, those neuron-related genes might be good diagnostic markers for oligodendroglioma of better prognosis as well.

Brain Pathol 2004;14:34-42.

INTRODUCTION

Gliomas are a major type of brain tumors, which constitute approximately one third of all primary brain tumors (11). Most gliomas have diffuse infiltrative trait, rendering surgical cure impossible and recurrence inevitable despite aggressive adjuvant treatment including radiotherapy and chemotherapy. Prognosis of each patient is determined primarily by the biological characteristics of tumor cells including response to treatment and rate of growth. Prediction of such biological characteristics of gliomas has been based on histological diagnosis which mainly relied on the morphological features of the tumor, and on the classification referring to the presumed origin of the tumor cells such as astrocytes, oligodendrocytes and ependymal cells. However, recent development in molecular genetic analysis have shown that even gliomas in a single histological entity can be divided into different subsets and may sometimes show different clinical features. A prominent example is that allelic loss of the short arm of chromosome 1 (1p), which is found in 60% to 80% of oligodendrogliomas, is closely associated with the chemosensitivity and longer survival (1, 8). Molecular biological background of such differences should be important information to be investigated which potentially leads to better management of gliomas, and one of powerful tools to do so is DNA microarray technology (5). Several studies have successfully demonstrated subtype specific genes in diffuse gliomas based on the expression profile analysis, and also showed that such molecular profiles could indeed help accurate prediction of clinical outcome (4, 6, 7, 17, 20, 21).

In a previous work, we have demonstrated that expression profiles of oligodendrogliomas with 1p loss are significantly different from other oligodendrogliomas, and numerous genes presumed to be related to neuronal cells are preferentially expressed in this specific subset (16). In this study, we asked whether this trait would still hold within a wider range of gliomas including astrocytic tumors. Such findings may not only be of diagnostic significance, but also would bring a new insight into glioma classification based on gene expression.

MATERIALS AND METHODS

Sample preparation. Tumor samples and paired blood samples were obtained at surgery after written informed consents. Consensus histological diagnoses were made on formalin-fixed paraffin-embedded tissues by four independent neuropathologists following the WHO classification (11). Loss of heterozygosity (LOH) assay on chromosomes 1p and 19q using microsatellite markers were performed as described previously (24). The frozen tumor sample was homogenized in Trizol (Invitrogen, Corp., Carlsbad, Calif) and total RNA was isolated following manufacturer's instructions. RNA was quantitated by ultraviolet absorbance at 260 and 280 nm and its quality was assessed by agarose gel electrophoresis.

GeneChip experiment. In addition to 2 normal brains, 6 oligodendrogliomas with 1pLOH (4 WHO grade II and 2 grade III cases), and 5 oligodendrogliomas without 1pLOH (4 grade II and 1 grade III cases) which were all reported in our previous study (16), 6 diffuse astrocytomas (grade II) and 5 glioblastomas (grade IV) were subjected to gene expression profile analysis. The high-density oligonucleotide arrays (GeneChip Human U95A array, Affymetrix, Santa Clara, Calif), which contain probe sets for approximately 12 626 human genes and ESTs, were used. Biotin-labeled cRNA was synthesized from aliquots (5 μg) of total RNA from each sample, and hybridization, washing, and detection of signals were carried out as described previously (9, 16). The Microarray Analysis Suite (MAS) 4.0 software (Affymetrix) was used to calculate the gene expression levels. The average background and noise (Raw Q) value calculated by MAS 4.0 were less than 241 (199 ± 26) and 7.13 (6.07 ± 0.78), respectively under 100% PMT setting. To allow comparison among multiple arrays, gene expression levels were normalized for each array by assigning the average of overall expression levels to be 100. The signal values of β-actin as an internal control showed <2-fold variation (4488 ± 576). The scaling factor used for all samples was 0.68 ± 0.18. The percentage of probe sets scored as detected ("Present") in each sample ranged from 48 ± 3% (42%-55%). These metrics demonstrate that the quality of each array is comparable. A value of 10 was assigned to every expression value below 10, because such low values are vulnerable to noise and artifacts.

Selection of subtype-specific genes. All glioma samples analyzed by GeneChip (N = 22) fall into 4 groups: oligodendroglial tumors with 1pLOH (n = 6), without 1pLOH (n = 5), low-grade astrocytomas (n = 6), and glioblastomas (n = 5). An ideal subtype-specific gene should have higher expression in samples of this subgroup and lower expression in samples of the other 3 types. For the selection of such genes, we used public software called Significant Analysis of Microarrays (SAM 1.21) (23), which is one of the methods to solve the statistical problem occurring in the analysis of large numbers of genes with small numbers of experiments. Basically, a score assigned by SAM is signal-to-noise (S/N) ratio called relative difference $d(i)$, which is calculated by $\{\mu_I(i)-\mu_U(i)\}/\{s(i)+s_0\}$ when $\mu_I(i)$ and $\mu_U(i)$ denote the average levels of expression for gene(i) in group I and U, respectively, and $s(i)$ is defined as the standard deviation of repeated expression measurements. Then, taking gene-specific fluctuations into account, SAM estimates the percentage of genes identified by chance as the false discovery rate (FDR) using permutations of the repeated measurements. SAM also identifies genes with statistically significant changes and score q-value, which is similar to the familiar "p-value."

Before SAM was applied, the control probes and genes called absent (not detected) by the expression algorithm in MAS 4.0 software or less than 100 in all 24 samples were excluded because of low confidence of scarcely expressed genes. Then by the pre-filtering, the 2756 probe sets whose maximum and minimum expression levels among 22 tumor samples differed by more than 100, and had more than 5-fold difference, were selected for the following statistical analysis.

Comparison with normal brain tissue data. To see expressions of the selected genes in normal brain tissues, we used Affymetrix U95A array expression data in the Gene Expression Atlas on the website of Genomics Institute of the Novartis Research Foundation (22), in addition to the data obtained from our two normal whole brain samples. This database contains 2 whole brain, a cerebral cortex, 2 cerebellum, 2 caudate nucleus, 2 amygdala, 2 thalamus, 3 corpus callosum and 2 spinal cord. These data were linearly scaled to the same target signal (100) as in our own expression data. After this conversion, the expression levels of internal control genes such as β-actin (4425 ± 1122) in these normal tissues were similar to our data. The average gene expression levels in our normal brains and those in downloaded samples (whole brain) were also well correlated (coefficient r = 0.88) among pre-filtered genes. Hierarchical clustering was carried out by the programs Cluster and TreeView using selected 80 subtype-specific genes (3).

Quantitative real-time PCR. Quantitative real-time PCR (qPCR) was performed using iCycler (Bio-Rad, Hercules, Calif). cDNA was synthesized with oligo-dT primer from 2 μg total RNA using SuperScript Preamplification System (Invitrogen). The aliquot of cDNA were amplified by Taq polymerase for 40 cycles, consisted of 15 seconds of denaturing at 94°C, 15 seconds of annealing at 63-70°C, and 30 seconds of extension at 72°C with monitoring of the SYBR Green I dye intercalation signal. Each PCR reaction was done in triplicate. For each sample, relative expression of a gene to the expression in reference cDNA mixture of several cell lines and tissues was calculated, and the expression of each gene was then normalized using β-*actin* expression of the same sample as an internal control. The following primer sets and annealing temperature (Tm) were used: forward (F) 5′-AGAAG GAGAT CACTG CCCTG GCACC-3′, reverse (R) 5′-CCTGC TTGCT GATCC ACATC TGCTG-3′ and Tm 65°C for β-*actin*; F 5′-AATTA TTTCG GGGCT CTGCG GAACC-3′, R 5′-GCACC TTGCT TCAGC TCTCA AAACG-3′ and Tm 67°C for *MYT1L*; F 5′-TACCA CCCGG TCCCC ACTTT ATTGC-3′, R 5′-TTCGG GCCAC CCCTA CTTCT TCTCC-3′ and Tm 63°C for *L1CAM*; F 5′-CAGAC TCTGG CAACA CCTGC AATGG-3′, R 5′-CACGG GCCCG GATGA TTTCT ACCTC-3′ and Tm 70°C for *RIMS2*; F 5′-GAAGT GGCCC AGGAA GCTGC TGAAG-3′, R 5′-CAGGG ACAGA ATTGT GCTGC TGGTG-3′ and Tm 70°C for *SNCB*; F 5′-GAGGA CCGTC ATCAG GCCGA CATTG-3′, R 5′-GGCCA TCTCC CACTT GGTGT TCCTC-3′ and Tm 70°C for *NEFH*; F 5′-CCCTT TCCCC AAAAG TAGCG TAACC-3′, R 5′-TTGAC AGGAC GGCGA CTGTG AGAC-3′ and Tm 68°C for *OLIG1*. The specificity of the amplification products was validated using post-amplification melt curve analysis. Differences of gene expression in oligodendroglioma with 1pLOH and the other gliomas were tested by Kruskal-Wallis analysis.

In situ hybridization. Tumor samples and adjacent normal brain tissue stored at -80°C were embedded into Tissue-Tek OCT compound (Sakura Finetek, Torrance, Calif) and cryosectioned (7-μm thick), and then fixed in 4% paraformaldehyde. For the detection of *MYT1L* mRNA, the sections were treated with proteinase K

GeneChip probe number	Genbank accession number	Gene	Symbol	Expression level†					Locus
				Oligodendroglioma		Astrocy-toma	GBM	Normal whole brain	
				1pLOH (+)	1pLOH (-)				
32712_at	AB029029	Myelin transcription factor 1-like *‡	MYT1L	125±70	13±5	20±19	10±0	203±102	2p
37210_at	S78296	Internexin neuronal intermediate filament protein α	INA	622±182	177±54	235±102	136±18	816±85	10q
34526_s_at	AF052108	Hypothetical protein LOC157627	LOC157627	154±77	30±15	39±50	11±2	272±120	8p
38551_at	U52112	L1 cell adhesion molecule *	L1CAM	479±273	58±62	44±46	73±43	620±167	Xq
41589_at	Y15065	Potassium voltage-gated channel, KQT-like	KCNQ2	119±86	32±25	10±0	10±0	325±146	20q
40234_at	X96484	DiGeorge syndrome critical region gene 6	DGCR6	443±209	258±167	19±21	59±60	439±175	22q
33426_at	Y00064	Chromogranin B (secretogranin 1)	CHGB	233±139	85±44	49±44	16±9	282±148	20p
32709_at	L39833	Potassium voltage-gated channel, shaker-related	KCNAB1	81±36	23±10	27±15	26±20	180±33	3q
37568_at	U79242	Clone 24816 mRNA sequence		97±33	20±10	44±15	30±11	140±22	
38163_at	AB018294	Regulating synaptic membrane exocytosis 2 *	RIMS2	133±58	29±14	39±33	11±2	140±58	8q
34520_at	AJ012582	Potassium voltage-gated channel, brain 2	HCN2	79±28	39±16	25±13	11±2	144±26	19p
36965_at	U13616	Ankyrin 3, node of Ranvier (ankyrin G)	ANK3	196±83	78±70	63±35	44±19	490±215	10q
38699_at	X00734	Tubulin beta 5	TUBB5	500±152	217±115	138±76	94±90	1785±282	19p
37580_at	AF036271	SH3-domain GRB2-like 3	SH3GL3	127±59	50±25	45±37	12±4	377±132	15q
39095_at	M58018	Myosin, heavy polypeptide 7, cardiac muscle, β	MYH7	95±79	20±13	14±8	18±10	10±0	14q
40733_f_at	D89377	Msh homeo box homolog 2	MSX2	79±33	32±5	30±5	36±6	31±24	5q
41675_at	AB014556	Synaptosomal-associated protein, 91kDa homolog	SNAP91	341±151	167±118	74±85	10±0	950±127	6q
38174_at	X99688	Pleckstrin and Sec7 domain protein	PSD	374±198	164±45	133±70	65±16	1068±259	10q
33947_at	U18550	G protein-coupled receptor 3	GPR3	112±20	50±24	32±23	38±15	133±39	1p
34788_at	AL049365	cDNA DKFZp586A0618		194±72	82±80	42±27	58±60	120±8	
37060_at	U79289	Clone 23695 mRNA sequence		72±35	22±2	32±16	27±8	215±30	
38855_s_at	D82343	Olfactomedin 1	OLFM1	762±599	236±56	222±215	143±114	2059±155	9q
180_at	S82470	Leukocyte receptor cluster (LRC) member 4	LENG4	74±33	29±17	23±15	22±8	121±74	19q
40653_at	U32439	Regulator of G-protein signaling 7	RGS7	133±32	43±15	59±32	61±37	371±61	1q
34527_r_at	AF052108	Hypothetical protein LOC157627	LOC157627	154±30	61±22	88±42	45±11	213±59	
41792_at	L78207	Sulfonylurea receptor	ABCC8	417±233	172±78	148±91	88±16	205±30	11p
37857_at	AL080188	MT-protocadherin	KIAA1775	141±61	68±22	48±33	17±9	48±15	10q
1998_i_at	U19599	BCL2-associated X protein	BAX	92±14	61±7	28±10	34±6	160±108	19q
40753_at	AF053136	Synuclein β*	SNCB	146±146	11±2	26±25	41±17	953±263	5q

Table 1. Highly expressed genes in oligodendroglioma with 1pLOH.
† Expression level of each gene was demonstrated as Mean ± S.E.M in each subgroup.
‡ The genes examined by qPCR are indicated by *.

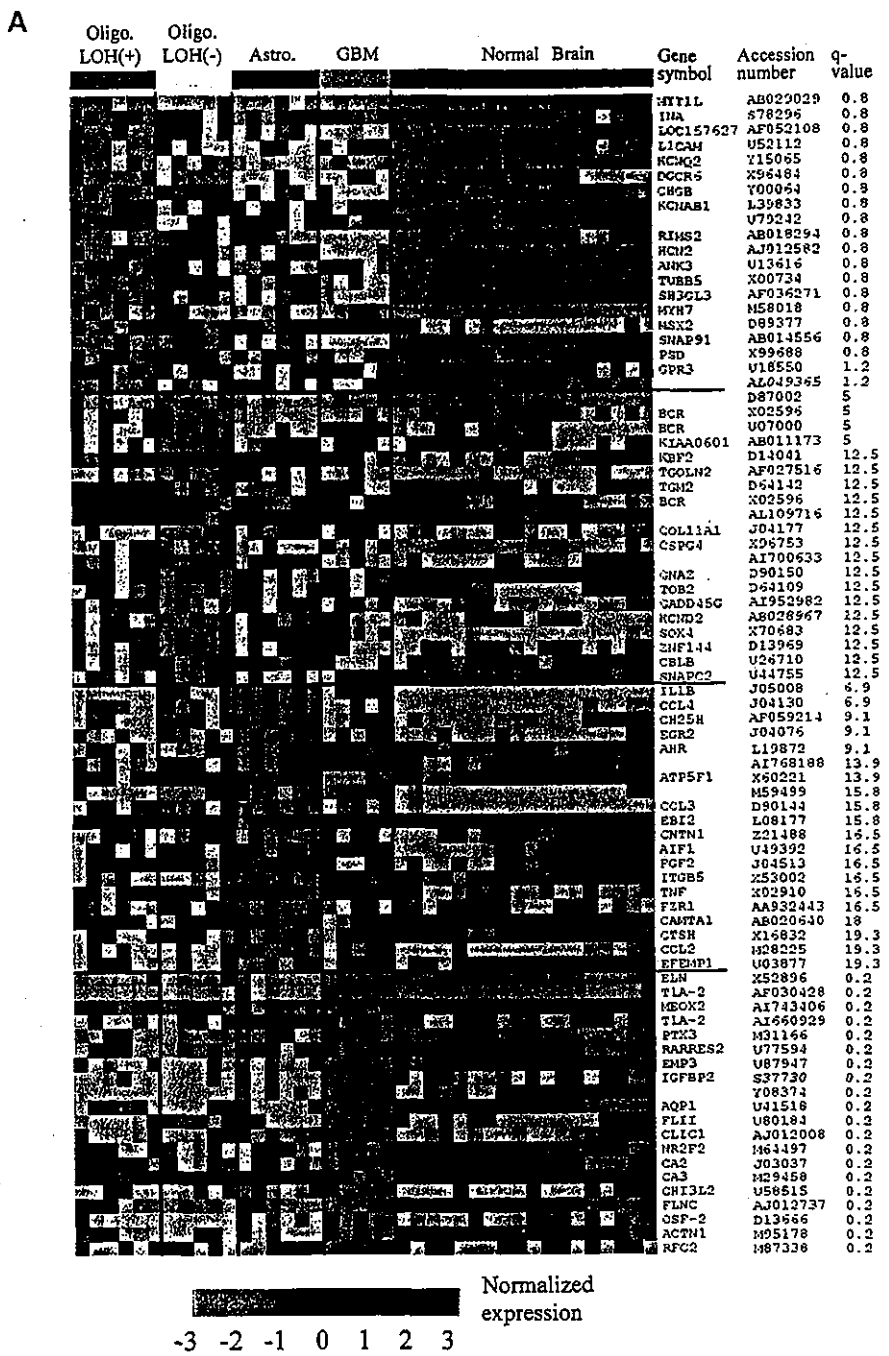

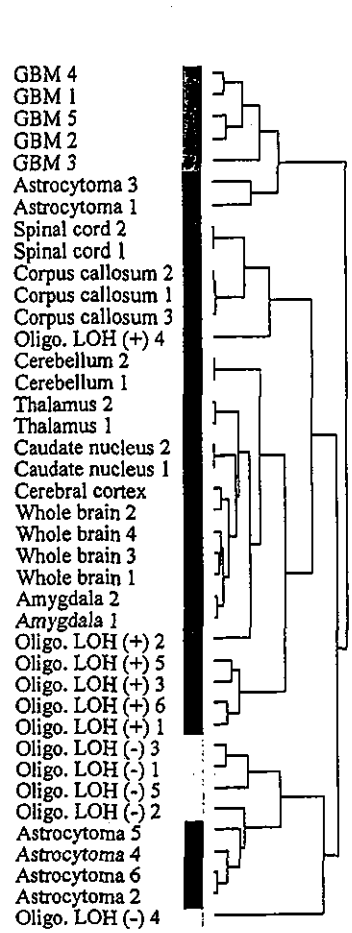

Figure 1. A. The genes characterizing 4 subgroups of diffuse gliomas. Each column represents a sample and each row represents a gene. Expression of each gene in 22 gliomas, together with 18 normal brain tissues was demonstrated in color gradation after normalization. Red indicates increased expression, and green indicates decreased gene expression. The order of samples are oligodendroglioma with 1pLOH (1-6), without 1pLOH (1-5), astrocytoma (1-6), glioblastoma (1-5), our whole brain (1, 2), downloaded whole brain (3, 4), cerebral cortex (1), cerebellum (1, 2), caudate nucleus (1, 2), amygdala (1, 2), thalamus (1, 2), corpus callosum (1-3) and spinal cord (1, 2). Note that the genes showing higher expression in oligodendroglioma with 1pLOH were also highly expressed in normal brain, except for corpus callosum and spinal cord. **B.** *The result of* hierarchical clustering using selected 80 subtype-specific genes. The oligodendrogliomas with 1pLOH were clustered into the same group with the normal brains, and were more similar to whole brain, cerebral cortex, cerebellum, caudate nucleus, amygdala and thalamus than corpus callosum and spinal cord. Two astrocytomas were clustered together with glioblastomas.

(code S3004; Dako, Glostrup, Denmark) diluted to 1:5000 at room temperature for 10 minutes, and 2 ng/μl of biotin-labeled oligonucleotide probe (antisense of 5′-ACATG GCTGT CACTG GATTT AGGCT TTCTG TCCTC C-3′ and sense of 5′-GGAGG ACAGA AAGCC TAAAT CCAGT GACAG CCATG T-3′) was hybridized at 37°C overnight. A GenPoint catalyzed signal amplification system (Dako) was used following manufacturer's instructions, and DAB substrate (Dako) was used to visualize amplified signal. The tissues were counterstained with hematoxylin. Furthermore, to test the quality of the mRNA in samples, positive and negative fluorescein-conjugated peptide nucleic acid (PNA) probes *against glyceraldehyde*

3-phosphate dehydrogenase, and PNA in situ hybridization detection kit (code K5201; Dako) were used according to the manufacturer's instruction.

Immunohistochemistry. Normal brain slides prepared simultaneously for in situ hybridization were immunolabeled. The slides were pretreated with microwave for total 20 minutes in citrate buffer pH 6.0, and then incubated with mouse anti-neuronal nuclei (NeuN) monoclonal antibody (Chemicon, Temecula, Calif) at 1:100 dilution for one hour at room temperature. A LSAB kit and a DAB substrate (DAKO) were used to visualize the antibody biding, and tissues were counterstained with hematoxylin.

RESULTS

The subtype-specific genes. SAM identified 29, 0, 0, and 247 subtype-specific genes with statistical significance of q-value <1.25% for oligodendroglioma with 1pLOH, without 1pLOH, astrocytoma and glioblastoma, respectively (highly expressed genes in oligodendroglioma with 1pLOH were listed in Table 1). Since SAM is applied 4 times to each subtype, the overall statistical significance for these genes is 5% after Benjamini correction for multiple testing. Then, we tried to select the same number of genes from each subtype of glioma for the subsequent clustering analysis, though SAM identified different number of genes as statistically significant. In this manuscript, main focus of our analysis was oligodendrogliomas with 1pLOH, in which 29 genes were identified as significantly highly expressed by SAM. On the other hand, genes list more than 20 in oligodendrogliomas without 1pLOH and astrocytoma had higher q-value and FDR. Therefore, we decided to select each 20 genes, which were sufficiently specific for oligodendroglioma with 1pLOH and glioblastoma, and were still acceptable for oligodendroglioma without 1pLOH and astrocytoma. Accordingly, we selected each 20 probe sets which showed lower q-value in each subgroup, as subtype-specific genes of oligodendroglioma with 1pLOH, without 1pLOH, astrocytoma and glioblastoma, of which median FDR were within 1.2, 12.5, 19 and 1.9 %, respectively (Figure 1A). Some of those genes showed consistency with other studies, such as insulin-like growth factor binding protein 2 (*IGFBP2*) whose higher expressions in glioblastoma were reported in the previous microarray studies (4, 20, 21).

Most of the genes that showed distinctively higher expression in oligodendroglioma with 1pLOH also showed similarly high expression in the normal brain, while the genes showing higher expression in other glioma subgroups did not have such a trend (Table 1, Figure 1A). Notably, many of those genes were considered to have neuron-related function. For example, myelin transcription factor 1-like (MYT1L) is thought to be a neuron specific transcription factor (10); internexin neuronal intermediate filament protein α (INA) may act as a neuron-specific intermediate filament protein (15); regulating synaptic membrane exocytosis 2 (RIMS2) and synaptosomal-associated protein 91kDa homolog (SNAP91) are supposed to be synapse related molecules; β-synuclein (SNCB) may play a role in neuronal plasticity and abundant in neurofibrillary lesions (2). L1 cell adhesion molecule (L1CAM), chromogranin B (CHGB), ankyrin 3 (ANK3), tubulin β5 (TUBB5), SH3-domain GRB2-like 3 (SH3GL3), pleckstrin and Sec7 domein protein (PSD), olfactomedin 1 (OLFM1), regulator of G-protein signaling 7 (RGS7), potassium voltage-gated channels such as KCNQ2, KCNAB1 and HCN2 are all thought to be expressed in neuronal cells. Besides those known genes, ESTs such as hypothetical protein LOC157627 and clone 23695 also seem to be abundantly expressed in the brain and neural tissue according to the public database such as UniGene, though their functions in the nervous system are not yet proven.

Using these 80 subtype-specific genes in total, clustering analysis was performed on the 22 tumors and 18 normal brain and spinal cord tissues (Figure 1B). The oligodendroglial tumors with 1pLOH were clustered into the same group with the normal brains, indicating their similarity in the expression pattern of the selected genes. Furthermore, oligodendroglioma with 1pLOH were more similar to whole brain, cerebral cortex, cerebellum, caudate nucleus, amygdala and thalamus than corpus callosum and spinal cord, possibly because corpus callosum and spinal cord consist mostly of glial cells than neurons. Two astrocytomas were clustered together with glioblastomas.

The validation studies using quantitative real-time PCR. Of the 29 genes that showed significantly higher expression in oligodendroglioma with 1pLOH, we selected four known genes for further validation study using qPCR. We also analyzed a gene for neurofilament heavy polypeptide (NEFH) which is known to be expressed in normal brain, and OLIG1 gene that is reported to be expressed specifically in oligodendrogliomas (12, 14). Forty-seven samples including 24 samples used in the microarray experiment and 23 additional gliomas were analyzed. The relative expression levels in qPCR of each six gene, *MYT1L*, *L1CAM*, *RIMS2*, *SNCB*, *NEFH* and *OLIG1* were shown in Figure 2. *MYT1L*, *L1CAM*, *RIMS2* and *SNCB* showed significantly higher expression in oligodendrogliomas with 1pLOH than other gliomas ($p<0.0001$, <0.005, <0.0001 and <0.001, respectively), and normal brains also had higher expression as expected from GeneChip data (Note that Y-axis in Figure 2 represents the relative gene expression level to the average expression in normal brain). We recognized, however, some exceptional cases (one of them was indicated by circle in Figure 2) that had higher expression of these genes in other glioma subgroups. Including such cases, gliomas showing higher expression in one of the 4 genes usually had similarly higher expression in other 3 genes as well. The expression levels of *NEFH* in gliomas were much lower than normal brain. *OLIG1* were highly expressed in gliomas comparing to normal brain, though it was not specific to oligodendrogliomas.

The results of qPCR corresponded well to the GeneChip data, and the correlation between the data from the qPCR and the GeneChip were 0.88 for *MYT1L*, 0.77 for *L1CAM*, 0.87 for *RIMS2*, and 0.98 for *SNCB* respectively, using Pearson correlation coefficient.

The expression of neuron-related molecules in oligodendroglioma with 1pLOH. To exclude the possibility of contaminated normal neurons as the source of the higher expression of neuronal genes in oligodendroglioma with 1pLOH, we performed in

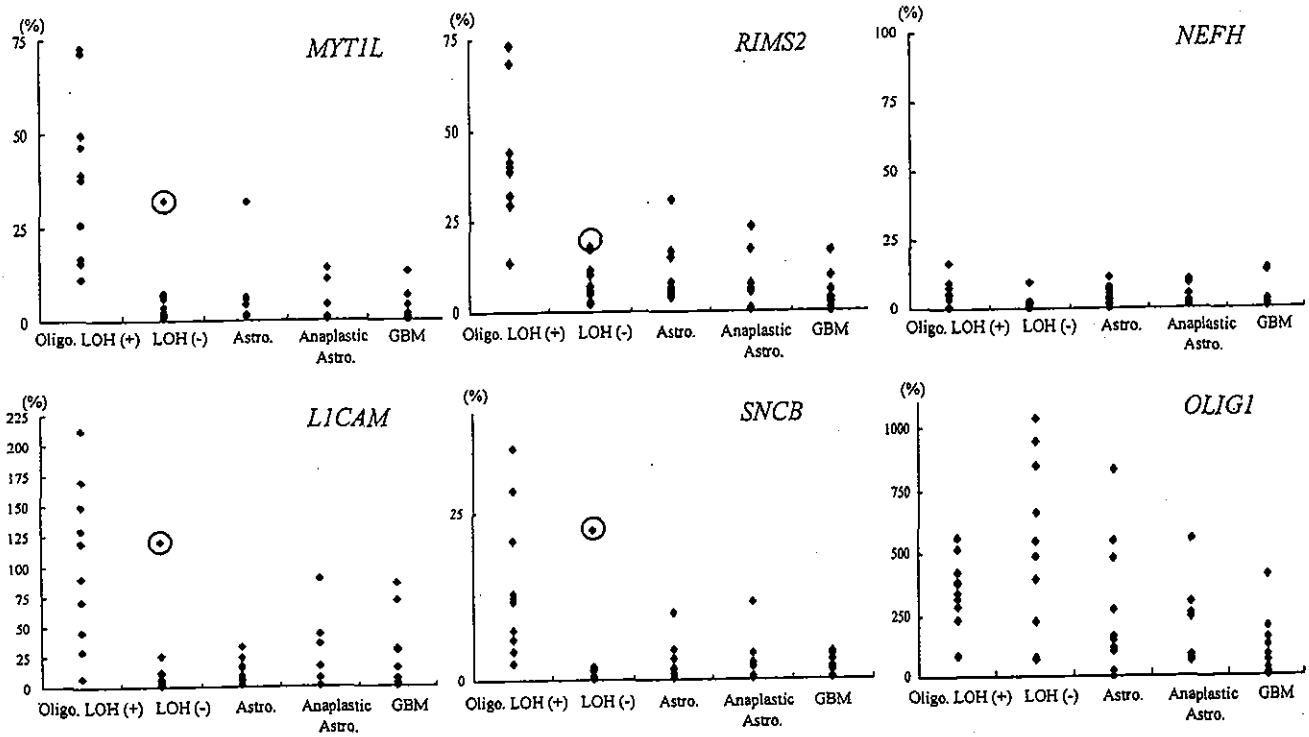

Figure 2. Quantitative real-time PCR analysis on oligodendrogliomas with 1pLOH (n=10), without 1pLOH (n=10), low-grade diffuse astrocytomas (n=9), anaplastic astrocytomas (n=7), glioblastomas (n=9) and normal brains (n =2). Note that Y-axis represents the relative gene expression level to the average expression in normal brains. *MYT1L*, *L1CAM*, *RIMS2* and *SNCB* showed significantly higher expression in oligodendrogliomas with 1pLOH than other gliomas ($p<0.0001$, <0.005, <0.0001 and <0.001, respectively) using the Kruskal-Wallis test. There were two exceptional cases; one oligodendrogliomas without 1p loss (indicated by circle) and one astrocytoma showed higher expression in those four genes. *NEFH* showed consistent lower expression in all glioma samples comparing with normal brain (<20%). Most of glioma samples had higher *OLIG1* expressions.

situ hybridization for *MYT1L* transcripts. Eleven samples containing good quality of mRNA confirmed by in situ hybridization using PNA probe as a positive control were evaluated; 2 normal brain tissues, 3 oligodendrogliomas with 1pLOH, 3 oligodendrogliomas without 1pLOH, 2 astrocytomas and 1 glioblastoma (Figure 3). *MYT1L* expressions were detected in 2 normal brain tissues and were highly expressed in cells containing large nuclei (Figure 3A, C). The cells containing large nuclei were also immunostained with anti-neuronal nuclei (NeuN) antibody and were assumed to be neurons (Figure 3A, inset). Expression of *MYT1L* transcripts was clearly demonstrated in 2 of 3 oligodendrogliomas with 1pLOH (Figure 3B, D), but not in oligodendrogliomas without LOH (Figure 3E), astrocytomas (Figure 3F) nor glioblastoma (Figure 3G).

DISCUSSION

In this study, we demonstrated that some of the genes showing higher expression in oligodendroglioma with 1p loss compared to the other major subtypes of gliomas were functionally neuron-related genes, with the expression at the similar levels in normal neurons. Although it was rather unexpected that neuron-related genes were expressed in gliomas, contamination of normal neurons in the samples of oligodendroglioma with 1p loss was not likely, because *i)* allelic losses observed on the microsatellite analysis were almost complete in all cases, indicating that the examined tissues consisted mostly of tumor cells, and *ii)* our in situ hybridization for *MYT1L* transcripts demonstrated that these genes were indeed expressed in the tumor cells. Furthermore, *iii)* expressions of other neuron specific genes expressed in normal brain tissues, such as gene encoding neurofilament subunit (*NEFH*, *NEFM* and *NEFL*), were much lower in oligodendrogliomas with 1p loss than those in normal brain. Therefore, the microarray analysis represented expression profile of the tumor cells, not normal neurons.

The qPCR analysis on several genes confirmed the microarray analysis results, and validated them on additional 23 gliomas samples. The results were mostly consistent, showing similar levels of higher expression in oligodendrogliomas with 1p loss but not in other gliomas. However, there were 2 exceptional cases; one oligodendroglioma without 1p loss and one astrocytoma showed higher expression in those genes. On re-reviewing the histology of those 2 tumors, we noticed that the oligodendroglioma case had occasional ependymoma-like portion, but the astrocytoma case was typical astrocytoma without any unusual morphology. We consider that these exceptional cases may reflect the heterogeneity of yet unknown background. To be noted was that the changes of expression levels of the genes were always to the same trend in all gliomas including the exceptional cases, suggesting a possible functional link among those genes.

We also compared WHO grade II (n = 8) and grade III (n = 3) oligodendrogliomas using Mann-Whitney test with cut-off p-values of 0.05, and 368 genes were detected as differentially expressed by grade (whole list of the selected genes would be available on request). Downregulated genes in grade III tumors included genes for CD44, alpha 1 syntrophin, connexin43 gap junction protein, CCAAT/enhancer binding protein delta, and chemokine receptor 4. Genes upregulated in grade III tumors included

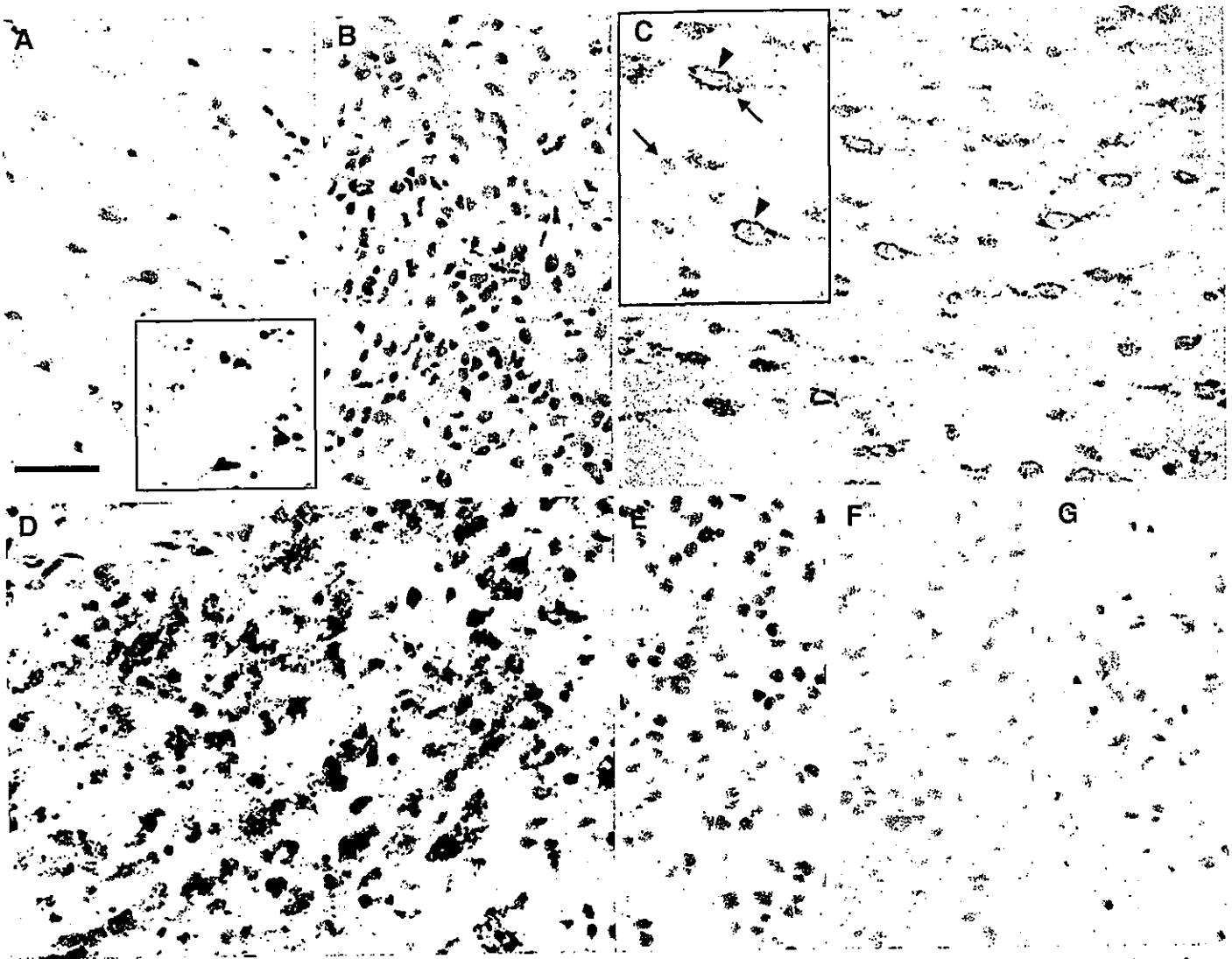

Figure 3. In situ hybridization for *MYT1L* transcripts, with corresponding H&E staining of normal brain (**A**) and oligodendroglioma with 1pLOH (**B**) on frozen section. *MYT1L* expressions were strongly observed in neurons (arrowheads), which contain large nuclei, comparing with the surrounding cells with small, round nuclei which were putatively considered as oligodendrocytes (arrows) (**C**). The cells containing large nuclei were also immunostained with anti-neuronal nuclei (NeuN) antibody (inset, **A**). Oligodendroglioma with 1pLOH actually expressed MYT1L transcripts (**D**), though oligodendroglioma without 1pLOH (**E**), astrocytoma (**F**) and glioblastoma (**G**) did not. (Bar=50 μm [A, B]; 30 μm [C, D, E, F, G]).

genes for myosin and interferon induced proteins. These genes listed above were concordant with previous report (25), suggesting the consistency of this DNA array analysis. However, further analysis of differentially expressed genes by tumor grade was not performed in this study, because statistical confidence for this data might be limited by small number of our grade III tumors.

Both Myt1 and its homologue Myt1l are zinc finger proteins of CCHC class that are expressed in neurons at early stages of differentiation. While Myt1 is expressed in cells of glial lineage, Myt1l is not detected in glial cells but co-expressed with Tuj1 in neurons around terminal mitosis (10). Therefore, Myt1l is supposed to play a role in the development of neurons. In our study, *MYT1L* was also expressed in neuron of normal adult human brain. The fact that oligodendroglioma with 1p loss express a subset of neuron specific genes like *MYT1L* would raise a question whether these tumor originate from the same glial progenitor cells as the other gliomas. Neurocytic differentiation and variable degrees of neuronal marker expression have been reported in oligodendrogliomas (19, 26, 27), and neuron-like physiological properties of oligodendroglioma cells have been observed as well (18). On the other hand, *OLIG1* and *OLIG2* genes, which are crucial in maturation of oligodendrocyte and its progenitor, were strongly expressed in oligodendrogliomas as previously reported 12, 14), although the expression of those 2 genes were not specific to oligodendrogliomas in our data. Therefore, these results together may suggest that oligodendroglioma with 1p loss have both neuronal and glial differentiation patterns at least on a certain group of genes. In line with such a still hypothetical proposition, recent studies indicated that some oligodendrocytes might share the same progenitor cells with neurons (13, 28).

Since the era of Baily and Cushing's inaugural works, classification of gliomas has been based upon hypothetical origins of the tumor, which were assigned to each tumor type according to their morphological features. With the rapid advancement in developmental biology of nervous system at the molecular level, such classifications could be reorganized using molecular markers related to neural development. Our

observations suggest that genetic subsets in gliomas may well be one of the subjects for such possible redefinition in the future. A clinically important question is whether these neuronal genes such as *MYT1L* could be used to identify more favorable subset of gliomas as diagnostic markers, independently to 1p loss. A recent report showed that in certain malignant gliomas, the expression profiling using microarray was successful in identifying a set of genes more accurate in predicting prognosis of patients than histological diagnosis (17). Notably, 2 patients of astrocytoma grade II which were clustered together with glioblastomas in our series (Figure 1B), indeed showed the clinical course equivalent to glioblastomas, suggesting usefulness of microarray for predicting patients' prognosis. However, almost all oligodendroglioma patients in the current study are still alive and therefore we do not have sufficient prognostic data for analysis at this point. Further investigation with more data, both in number of cases and length of follow-up, would certainly answer such question in the future.

ACKNOWLEDGMENTS

This work was supported by a Grants-in-Aid from the Ministry of Education, Culture, Sports, Science and Technology, Japan (No. 11671357 and No. 13470184). This study was carried out as a part of The Technology Development for Analysis of Protein Expression and Interaction in Bioconsortia on R&D of New Industrial Science and Technology Frontiers which was performed by Industrial Science, Technology and Environmental Policy Bureau, Ministry of Economy, Trade and Industry, and entrusted by New Energy Development Organization (NEDO).

We thank Drs Yoichi Nakazato, Takanori Hirose, Nobuaki Funata, and Junko Hirato for reviewing the histology. We also thank Drs Masato Nakafuku and Tetsuya Taga for helpful discussion of the manuscript. We thank expert help of Dr Hirokazu Taniguchi, Kaori Shiina for histological studies, and Reiko Matsuura, Chizu Kobayashi, Hiroko Meguro, Erio Ashihara, Saori Fukui and Junko Yagi for their technical assistance.

REFERENCES

1. Cairncross JG, Ueki K, Zlatescu MC, Lisle DK, Finkelstein DM, Hammond RR, Silver JS, Stark PC, Macdonald DR, Ino Y, Ramsay DA, Louis DN (1998) Specific genetic predictors of chemotherapeutic response and survival in patients with anaplastic oligodendrogliomas. *J Natl Cancer Inst* 90:1473-1479.

2. Clayton DF, George JM (1998) The synucleins: a family of proteins involved in synaptic function, plasticity, neurodegeneration and disease. *Trends Neurosci* 21:249-254.

3. Eisen MB, Spellman PT, Brown PO, Botstein D (1998) Cluster analysis and display of genome-wide expression patterns. *Proc Natl Acad Sci U S A* 95:14863-14868.

4. Fuller GN, Rhee CH, Hess KR, Caskey LS, Wang R, Bruner JM, Yung WK, Zhang W (1999) Reactivation of insulin-like growth factor binding protein 2 expression in glioblastoma multiforme: a revelation by parallel gene expression profiling. *Cancer Res* 59:4228-4232.

5. Golub TR, Slonim DK, Tamayo P, Huard C, Gaasenbeek M, Mesirov JP, Coller H, Loh ML, Downing JR, Caligiuri MA, Bloomfield CD, Lander ES (1999) Molecular classification of cancer: class discovery and class prediction by gene expression monitoring. *Science* 286:531-537.

6. Gutmann DH, Hedrick NM, Li J, Nagarajan R, Perry A, Watson MA (2002) Comparative gene expression profile analysis of neurofibromatosis 1-associated and sporadic pilocytic astrocytomas. *Cancer Res* 62:2085-2091.

7. Huang H, Colella S, Kurrer M, Yonekawa Y, Kleihues P, Ohgaki H (2000) Gene expression profiling of low-grade diffuse astrocytomas by cDNA arrays. *Cancer Res* 60:6868-6874.

8. Ino Y, Betensky RA, Zlatescu MC, Sasaki H, Macdonald DR, Stemmer-Rachamimov AO, Ramsay DA, Cairncross JG, Louis DN (2001) Molecular subtypes of anaplastic oligodendroglioma: implications for patient management at diagnosis. *Clin Cancer Res* 7:839-845.

9. Ishii M, Hashimoto S, Tsutsumi S, Wada Y, Matsushima K, Kodama T, Aburatani H (2000) Direct comparison of GeneChip and SAGE on the quantitative accuracy in transcript profiling analysis. *Genomics* 68:136-143.

10. Kim JG, Armstrong RC, v Agoston D, Robinsky A, Wiese C, Nagle J, Hudson LD (1997) Myelin transcription factor 1 (Myt1) of the oligodendrocyte lineage, along with a closely related CCHC zinc finger, is expressed in developing neurons in the mammalian central nervous system. *J Neurosci Res* 50:272-290.

11. Kleihues P, Cavenee WK (eds.) (2000) *Pathology and Genetics of Tumours of the Nervous System.* IARC Press, Lyon.

12. Lu QR, Park JK, Noll E, Chan JA, Alberta J, Yuk D, Alzamora MG, Louis DN, Stiles CD, Rowitch DH, Black PM (2001) Oligodendrocyte lineage genes (OLIG) as molecular markers for human glial brain tumors. *Proc Natl Acad Sci U S A* 98: 10851-10856.

13. Lu QR, Sun T, Zhu Z, Ma N, Garcia M, Stiles CD, Rowitch DH (2002) Common developmental requirement for Olig function indicates a motor neuron/oligodendrocyte connection. *Cell* 109: 75-86.

14. Marie Y, Sanson M, Mokhtari K, Leuraud P, Kujas M, Delattre JY, Poirier J, Zalc B, Hoang-Xuan K (2001) OLIG2 as a specific marker of oligodendroglial tumour cells. *Lancet* 358:298-300.

15. McGraw TS, Mickle JP, Shaw G, Streit WJ (2002) Axonally transported peripheral signals regulate alpha-internexin expression in regenerating motoneurons. *J Neurosci* 22:4955-4963.

16. Mukasa A, Ueki K, Matsumoto S, Tsutsumi S, Nishikawa R, Fujimaki T, Asai A, Kirino T, Aburatani H (2002) Distinction in gene expression profiles of oligodendrogliomas with and without allelic loss of 1p. *Oncogene* 21:3961-3968.

17. Nutt CL, Mani DR, Betensky RA, Tamayo P, Cairncross JG, Ladd C, Pohl U, Hartmann C, McLaughlin ME, Batchelor TT, Black PM, von Deimling A, Pomeroy SL, Golub TR, Louis DN (2003) Gene expression-based classification of malignant gliomas correlates better with survival than histological classification. *Cancer Res* 63: 1602-1607.

18. Patt S, Labrakakis C, Bernstein M, Weydt P, Cervos-Navarro J, Nisch G, Kettenmann H (1996) Neuron-like physiological properties of cells from human oligodendroglial tumors. *Neuroscience* 71:601-611.

19. Perry A, Scheithauer BW, Macaulay RJ, Raffel C, Roth KA, Kros JM (2002) Oligodendrogliomas with neurocytic differentiation. A report of 4 cases with diagnostic and histogenetic implications. *J Neuropathol Exp Neurol* 61:947-955.

20. Rickman DS, Bobek MP, Misek DE, Kuick R, Blaivas M, Kurnit DM, Taylor J, Hanash SM (2001) Distinctive molecular profiles of high-grade and low-grade gliomas based on oligonucleotide microarray analysis. *Cancer Res* 61:6885-6891.

21. Sallinen SL, Sallinen PK, Haapasalo HK, Helin HJ, Helen PT, Schraml P, Kallioniemi OP, Kononen J (2000) Identification of differentially expressed genes in human gliomas by DNA microarray and tissue chip techniques. *Cancer Res* 60:6617-6622.

22. Su AI, Cooke MP, Ching KA, Hakak Y, Walker JR, Wiltshire T, Orth AP, Vega RG, Sapinoso LM, Moqrich A, Patapoutian A, Hampton GM, Schultz PG, Hogenesch JB (2002) Large-scale analysis of the human and mouse transcriptomes. *Proc Natl Acad Sci U S A* 99:4465-4470.

23. Tusher VG, Tibshirani R, Chu G (2001) Significance analysis of microarrays applied to the ionizing radiation response. *Proc Natl Acad Sci U S A* 98:5116-5121.

24. Ueki K, Nishikawa R, Nakazato Y, Hirose T, Hirato J, Funada N, Fujimaki T, Hojo S, Kubo O, Ide T, Usui M, Ochiai C, Ito S, Takahashi H, Mukasa A, Asai A, Kirino T (2002) Correlation of histology and molecular genetic analysis of 1p, 19q, 10q, TP53, EGFR, CDK4, and CDKN2A in 91 astrocytic and oligodendroglial tumors. *Clin Cancer Res* 8: 196-201.

25. Watson MA, Perry A, Budhjara V, Hicks C, Shannon WD, Rich KM (2001) Gene expression profiling with oligonucleotide microarrays distinguishes World Health Organization grade of oligodendrogliomas. *Cancer Res* 61:1825-1829.

26. Wharton SB, Chan KK, Hamilton FA, Anderson JR (1998) Expression of neuronal markers in

oligodendrogliomas: an immunohistochemical study. *Neuropathol Appl Neurobiol* 24:302-308.

27. Wolf HK, Buslei R, Blumcke I, Wiestler OD, Pietsch T (1997) Neural antigens in oligodendrogliomas and dysembryoplastic neuroepithelial tumors. *Acta Neuropathol (Berl)* 94:436-443.

28. Zhou Q, Anderson DJ (2002) The bHLH transcription factors OLIG2 and OLIG1 couple neuronal and glial subtype specification. *Cell* 109:61-73.

Brain Tumor Pathol (2004) 21:53–56
DOI 10.1007/s10014-004-0154-1

SPECIAL ARTICLE

Ryo Nishikawa · Tatsuya Sugiyama · Yoshitaka Narita
Frank Furnari · Webster K. Cavenee · Masao Matsutani

Immunohistochemical analysis of the mutant epidermal growth factor, ΔEGFR, in glioblastoma

Received and accepted: February 5, 2004

Abstract The naturally occurring mutated form of the epidermal growth factor receptor, ΔEGFR (also named EGFRvIII and de2-7EGFR), greatly enhances glioblastoma (GBM) cell growth in vivo through several activities, such as down-regulating p27 and up-regulating *BclX(L)* while increasing signaling through the RAS-MAPK and PI3-K cascades. More than half of GBMs, especially of the de novo type, overexpress EGFR, and 50%–70% of these express ΔEGFR. However, little is known about the distribution of ΔEGFR-expressing tumor cells within surgical specimens. In order to address this clinically important issue, we performed immunohistochemical analyses of 53 GBMs obtained during surgery using the anti- ΔEGFR monoclonal antibody, DH8.3. We also simultaneously analyzed wild-type EGFR expression in these tissues using the anti-EGFR monoclonal antibody, EGFR.113. ΔEGFR and wild-type EGFR expression were observed in 20/53 (38%) and 29/53 (55%), respectively. Nineteen (95%) of the ΔEGFR-positive tumors also expressed wild-type EGFR; one case was ΔEGFR-positive but wild-type EGFR-negative. In 13/20 (65%) of the ΔEGFR-positive tumors, tumor cells were scattered diffusely within the tumors, 6/20 showed geographical distribution of ΔEGFR-positive tumor cells, and one case showed homogeneous staining. In the wild-type EGFR-positive cases, almost all tumor cells expressed EGFR. The differential distribution of cells expressing the two receptors observed here may suggest either that ΔEGFR arises at a low frequency from wild-type EGFR-expressing cells, perhaps during the process of gene amplification, or that there is a paracrine-type of interaction between them.

Key words Epidermal growth factor receptor · Glioblastoma · Immunohistochemistry

R. Nishikawa (✉) · T. Sugiyama · M. Matsutani
Department of Neurosurgery, Saitama Medical School, 38 Morohongo, Moroyama-machi, Iruma-gun, Saitama 350-0495, Japan
Tel. +81-49-276-1334; Fax +81-49-294-4955
e-mail: rnishika@saitama-med.ac.jp

Y. Narita · F. Furnari · W.K. Cavenee
Ludwig Institute for Cancer Research, San Diego, CA, USA

W.K. Cavenee
Department of Medicine, Center for Molecular Genetics and Cancer Center, University of California at San Diego, La Jolla, CA, USA

Indroduction

The epidermal growth factor receptor (EGFR) gene is amplified at the DNA level and overexpressed at the level of mRNA or protein expression in tumor tissues of about 40%–50% of human glioblastoma (GBM) cases.[1–3] This EGFR gene amplification is often followed or accompanied by further gene rearrangement. About two-thirds of such rearrangements result in a particular mutant form called ΔEGFR, de2-7EGFR, or EGFRvIII, an in-frame deletion of exons 2–7 resulting in a deletion of 267 amino acids.[4–6] The resulting mutant protein is ligand independent, constitutively phosphorylated, and localized primarily to the cell surface.[7–9] ΔEGFR promotes the tumorigenesis of GBM cells in vivo by increasing cellular proliferation,[10] decreasing cellular apoptosis,[11] and promoting tumor cell invasion.[12] However, these conclusions have derived from the analysis of the behavior of xenografts that arose after inoculation of cells expressing relatively homogeneous levels of ΔEGFR, and little is known about the distribution of ΔEGFR-expressing tumor cells in surgical specimens. Since this limits understanding of the clinical significance of ΔEGFR, we performed immunohistochemical analysis of ΔEGFR and wild-type EGFR expression in primary GBM tissues. Our results revealed differential distribution of tumor cells expressing these receptors, suggesting potential interactions between them.

Materials and methods

Brain tumor samples

Fifty-three GBM specimens that were surgically resected between 1989 and 2002 at Saitama Medical School were subjected to investigation. All tumors were diagnosed according to the World Health Organization (WHO) classification of brain tumors.[13] Tissue samples were fixed in 10% formalin and embedded in paraffin for histological as well as immunohistochemical examination. For Western blotting, samples were snap-frozen in liquid nitrogen in the operating rooms and stored at −80°C until use. Twenty samples were available for this series of studies.

Immunohistochemistry

The sections were deparaffinized, rehydrated, and incubated in hydrogen peroxide to block endogenous peroxidase activity, followed by antigen retrieval in a steam cooker and preincubation in normal goat serum. An anti-ΔEGFR monoclonal antibody, DH8.3, raised against a synthetic peptide spanning the unique junctional sequence of the deleted part of ΔEGFR,[14] was diluted 1:50 and applied to the samples for 1 h at room temperature. DH8.3 does not react with wild-type EGFR.[14] A standard ABC method was performed according to the manufacturer's recommendations (Vectastain, Vector Laboratories, Burlingame, CA, USA), and diaminobenzidine tetrahydrochloride was used to visualize the immunoreactivities. The slides were lightly counterstained with hematoxylin. Anti-EGFR monoclonal antibody, EGFR.113, raised against the extracellular domain of the wild-type EGFR was purchased from Novocastra (Newcastle, UK) and used for immunohistochemistry according to the manufacturer's recommendations.

Western blotting

The tissue specimens were lysed in extraction buffer (50 mM Tris-HCl [pH 7.6], 50 mM NaCl, 2% NP-40, 0.5% deoxycholic acid, 0.2% sodium dodecyl sulfate [SDS], 1 mM phenylmethylsulfonyl fluoride, 5 μg/ml leupeptin, 5 μg/ml aprotinin, and 0.5 mM Na_3VO_4) and sonicated. The lysates were centrifuged at 8000 *g* for 5 min, and the supernatants were collected. Each protein sample (20 μg) was separated with 7.5% polyacrylamide/SDS gels and electroblotted onto nitrocellulose membranes (ECL membrane, Amersham Pharmacia Biotech, Piscataway, NJ, USA). After blocking with 5% skim milk in Tris-buffered saline with 0.05% Tween 20, the membranes were incubated with an anti-EGFR monoclonal antibody, C13, which reacts with both wild-type EGFR and ΔEGFR (a kind gift from Dr. Gordon Gill, University of California at San Diego), and then incubated with a horseradish peroxidase-conjugated antimouse secondary antibody (Vector Laboratories), and subjected to chemiluminescence detection (ECL, Amersham Pharmacia Biotech).

Image intensification

The images from immunohistochemistry and Western blotting were captured with a digital camera and processed with Adobe Photoshop 7.0 on an Apple Macintosh computer.

Results

Immunohistochemistry

Positive immunoreactivities for DH 8.3 and EGFR.113 were observed in 20/53 (38%) and 29/53 (55%), respectively. Of those 20 cases positive for DH8.3, 19 were also positive and 1 was negative for EGFR.113. Typical examples of DH8.3-immunoreactivity are shown in Fig. 1A–E. Immunoreactivities for DH8.3 were observed on the cell membrane or in the cytoplasm of tumor cells that were similar to those for EGFR.113 (Fig. 1A and F). Immunoreactive cells were scattered diffusely in the 13 of 20 (65%) specimens positive for DH8.3 (Fig. 1A and B). In six specimens (30%), cells immunoreactive for DH8.3 were geographically distributed (Fig. 1C). The remaining specimen showed a homogeneous distribution of immunoreactive cells. In one specimen, DH8.3-immunoreactive cells were observed adhering to tumor vessels (Fig. 1D and E). On the other hand, in the tumors immunoreactive for EGFR.113, almost all tumor cells had homogeneous immunoreactivities, as shown in Fig. 1F, except for one case that showed geographical distribution of EGFR-expressing cells. Figure 1F is from the same area of the same specimen shown in Fig. 1B.

Western blotting

Significant amounts of ΔEGFR and full-length EGFR were detected in 9 of 20 (45%; lanes 5, 6, 8, 9, 10, 11, 13, 17, and 20 in Fig. 2) and 12 of 20 (60%; lanes 2, 5, 6, 7, 8, 9, 10, 11, 13, 15, 17, and 20 in Fig. 2) samples by Western blotting, respectively. Three samples (lanes 2, 11, and 15 in Fig. 2) were negative for EGFR.113 by immunohistochemistry but positive for full-length EGFR by Western blotting. None of the samples negative for full-length EGFR by Western blotting was positive for EGFR.113 by immunohistochemistry, and both results were concordant in 17/20 (85%) of the samples. Four samples (lanes 5, 9, 11, and 17 in Fig. 2) were negative for DH8.3 by immunohistochemistry and positive for ΔEGFR by Western blotting, and both results were concordant in 16/20 (80%).

Discussion

Expression of ΔEGFR was observed in 20/53 (38%) of GBM samples by immunohistochemistry and 9/20 (45%) by Western blotting. Those frequencies were similar to those

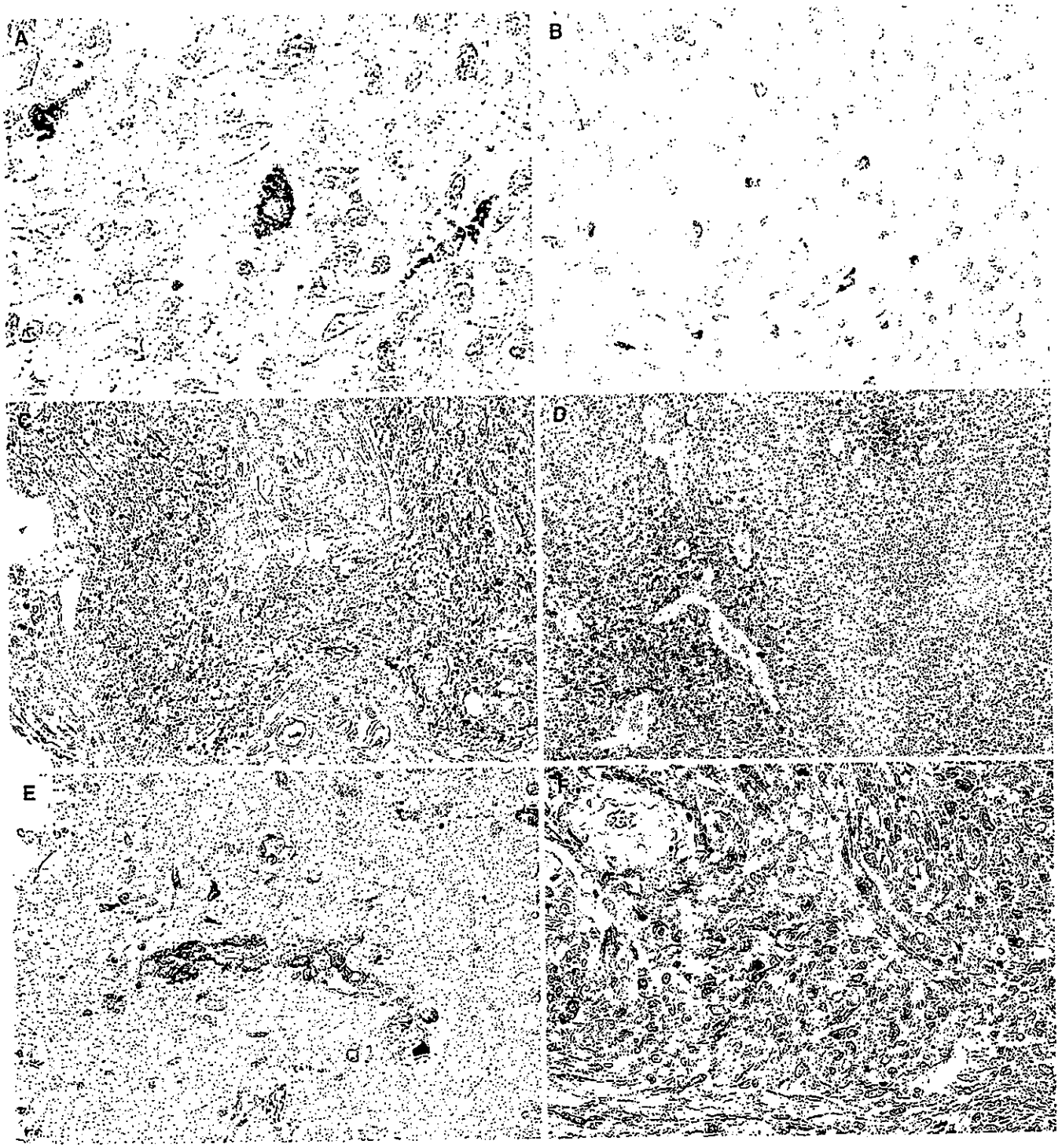

Fig. 1. Immunohistochemical detection of mutated epidermal growth factor receptor (ΔEGFR) (**A–E**) and wild-type EGFR (**F**) expression in glioblastoma specimens. Original magnifications are (**A**) ×1000, (**B, C, E, F**) ×400, and (**D**) ×100

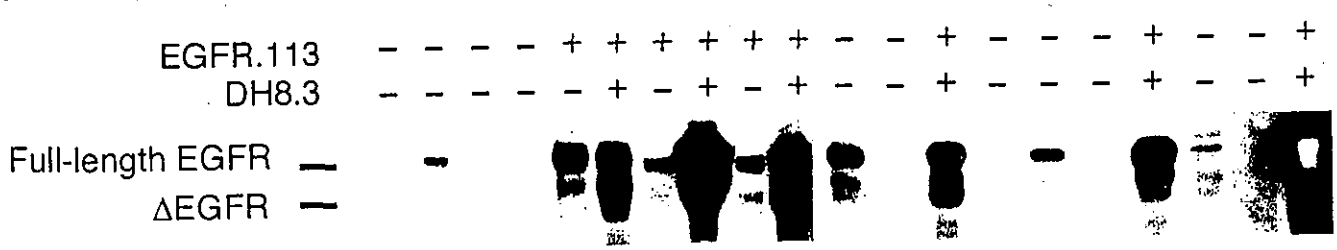

Fig. 2. Western blotting analysis of *ΔEGFR* and wild-type *EGFR* expression in glioblastoma specimens. + or − indicates immunoreactivities for *DH8.3* and *EGFR.113* by immunohistochemistry

in reported series: 7/12 (58%) by Western blotting,[5] and 8/12 (67%)[5] or 12/21 (62%)[4] by immunohistochemistry. Among the 20 cases in which frozen samples were available for Western blotting, the results of Western blotting and immunohistochemistry were concordant in 16 cases (80%). Expression of ΔEGFR in the remaining four cases was positive by Western blotting but negative by immunohistochemistry, which would indicate either that Western blotting was more sensitive for the detection of low levels of ΔEGFR expression, or that there were sampling errors due to the heterogeneous location of positive cells.

Each of the 20 cases that were immunoreactive for DH8.3 by immunohistochemistry was also immunoreactive for EGFR.113, with one exception. Among the 29 cases positive for EGFR.113, 19 (66%) were positive for DH8.3. It has been reported that GBMs with ΔEGFR mutation always harbor increased *EGFR* gene dosage, and frequency of ΔEGFR found in GBMs with *EGFR* amplification was 67%.[6] These data suggest that amplification of the *EGFR* gene precedes *EGFR* mutation.

GBM cells expressing ΔEGFR have a remarkable in vivo growth advantage.[7] One consequence of this could be a clonal expansion of the cell population. Consonant with this notion are reported experiments showing that injection of a mixture of U87MG.ΔEGFR (a GBM cell line expressing ΔEGFR) and parental U87MG at a 1:50000 ratio into nude mouse brains showed an outgrowth of U87MG.ΔEGFR cells, with the proportion reaching 83% in the tumors that developed.[11] The geographical distribution of ΔEGFR-expressing tumor cells observed in surgical specimens has been believed to be the result of an analogous clonal expansion. However, our results here show that GBM tumor cells expressing ΔEGFR prefer to distribute diffusely in a scattering pattern in the majority of cases. In contrast, tumor cells expressing wild-type EGFR appeared to distribute in a more homogeneous fashion (Fig. 1F). The differential distribution of ΔEGFR- and wild-type EGFR-expressing tumor cells, together with the fact that almost all tumors expressing ΔEGFR expressed wild-type EGFR, appears to support the hypothesis that ΔEGFR arises at a low frequency from wild-type EGFR-expressing cells. The significantly enhanced biological aggressiveness of the tumor cells expressing ΔEGFR, together with their often diffuse occurrence among other tumor cells, also raises the possibility that they might provide a positive field effect on surrounding tumor cells that overexpress wild-type EGFR. The nature of such interactions requires further study.

Acknowledgments We thank Ms. Naoko Teshima for her excellent technical assistance. This work was supported in part by grants from the National Cancer Institute, NIH and the National Foundation for Cancer Research (both to WKC).

References

1. Wong AJ, Bigner SH, Bigner DD, et al (1987) Increased expression of the epidermal growth factor receptor gene in malignant gliomas is invariably associated with gene amplification. Proc Natl Acad Sci USA 84:6899–6903
2. Ekstrand AJ, Sugawa N, James CD, et al (1992) Amplified and rearranged epidermal-growth-factor-receptor genes in human glioblastomas reveal deletions of sequences encoding portions of the N- and/or C-terminal tails. Proc Natl Acad Sci USA 89:4309–4313
3. Simmons ML, Lamborn KR, Takahashi M, et al (2001) Analysis of complex relationships between age, p53, epidermal growth factor receptor, and survival in glioblastoma patients. cancer Res 61:1122–1128
4. Wikstrand CJ, Hale LP, Batra SK, et al (1995) Monoclonal antibodies against EGFRvIII are tumor specific and react with breast and lung carcinoma and malignant gliomas. Cancer Res 55:3140–3148
5. Feldkamp MM, Lala P, Lau N, et al (1999) Expression of activated epidermal growth factor receptors, Ras-guanosine triphosphate, and mitogen-activated protein kinase in human glioblastoma multiforme specimens. Neurosurgery 45:1441–1453
6. Frederick L, Wang X-Y, Eley G, et al (2000) Diversity and frequency of epidermal growth factor receptor mutations in human glioblastomas. Cancer Res 60:1383–1387
7. Nishikawa R, Ji XD, Harmon RC, et al (1994) A mutant epidermal growth factor receptor common in human glioma confers enhanced tumorigenicity. Proc Natl Acad Sci USA 91:7727–7731
8. Huang H-JS, Nagane M, Klingbeil CK, et al (1997) The enhanced tumorigenic activity of a mutant epidermal growth factor receptor common in human cancers is mediated by threshold levels of constitutive tyrosine phosphorylation and unattenuated signaling. J. Biol Chem 272:2027–2935
9. Wikstrand CJ, McLendon RE, Friedman AH, et al (1997) Cell surface localization and density of the tumor-associated variant of the epidermal growth factor receptor, EGFRvIII. Cancer Res 57: 4130–4140
10. Narita Y, Nagane M, Mishima K, et al (2002) Mutant epidermal growth factor receptor signaling down-regulates p27 through activation of the phosphatidylinositol 3-kinase/Akt pathway in glioblastomas. Cancer Res 62:6764–6769
11. Nagane M, Coufal F, Lin H, et al (1996) A common mutant epidermal growth factor receptor confers enhanced tumorigenicity on human glioblastoma cells by increasing proliferation and reducing apoptosis. Cancer Res 56:5079–5086
12. Lal A, Glazer CA, Martinson HM, et al (2002) Mutant epidermal growth factor receptor up-regulates molecular effectors of tumor invasion. Cancer Res 62:3335–3339
13. Kleihues P, Burger PC, Collins VP, et al (2000) Glioblastoma. In: Kleihues P, Cavenee WK (eds) Pathology and genetics of tumours of the nervous system. IARC, Lyon, pp 29–39
14. Hills D, Rowlinson-Busza G, Gullick WJ (1995) Specific targeting of a mutant, activated EGF receptor found in glioblastoma using a monoclonal antibody. Int J Cancer 63:537–543

Cell Biology of Brain Tumor : With Special Emphasis on Tumor Cell Invasion

Takamitsu Fujimaki, M.D., Ph.D.

Department of Neurosurgery, Teikyo University School of Medicine, Tokyo, Japan

Introduction

Treatment results of malignant tumors of various organs have been progressing. The 5-year survival rate as well as cure rate have been improved. The treatment results of malignant brain tumors, however, have not improved dramatically with some exceptions such as medulloblastoma and germ cell tumors. The results of gliomas, especially glioblastoma, are extremely poor. In this report, the research history of malignant brain tumors is reviewed stressing importance of cell biological standpoint.

To establish glioma, there are many steps such as initiation of tumor with genetic changes, tumor establishment escaping from immune system, tumor progression with proliferation of cells and angiogenesis, finally invasion to surrounding tissue. All of these steps are the target for malignant brain tumor research and therapy.

Recent advancement of molecular biology and genetic study of glial tumors are remarkable. However these advancements do not directly mean the improvement of treatment, but also does not have good correlation with clinical situations. The most important point which we should focus on is that the tumor cells exist in the host (patient) in the context of host-tumor interaction. Thus even in the era of major advancement in molecular biology, pathology as well as cell biology are important target to study in the neuro-oncology research. In this brief review, cell biological aspects of malignant glioma will be discussed.

Historical Aspect of Research of Proliferative Potential of Malignant Brain Tumor

Biology of glioma has been studied from the standpoint of growth potential. Hoshino and his colleagues opened and developed this field.[17,18] Based on their and other investigators, it is known that in glioma tissue, proliferating tumor cells are recruited from G0 (resting) cells. Irrespective of grade of the tumor, the cell cycle time of glioma is in a narrow range. Thus the ratio of proliferating cells represents the potential of tumor proliferation itself.[23,29] Historically this study of proliferation was initiated with autoradiography using ^{3}H-thymidine.[17] Then bromodeoxyuridine (BrdU, BudR) as thymidine analogue was used widely. BrdU was given to the patients before excision of the tumor or the tumor tissue was incubated in a medium containing BrdU immediately after tumor excision. Cells which are synthesizing DNA (in S phase) incorporate BrdU and incorporated BrdU was stained using monoclonal antibody. Thus cells in S phase can be differentiated from other cells. The S phase labeling index (LI) of each tumor was counted and their proliferative potential was studied.[23] Later this method was replaced by Ki67 staining or MIB-1 staining which stains all the cells in cell cycle.[11] With these approaches, biological behavior of gliomas were gradually disclosed, i.e,

S phase labeling index and its correlation to prognosis of patients.[16,12] Sensitivity to radiation therapy was also assessed by looking at the viable cells after radiation therapy. These methodology are called cell kinetics.

Resistance to Radiation Therapy

Gliomas are radioresistant. Irrespective of intensive radiation therapy, glioblastoma cannot be controlled for longer period. Cell kinetics study of glioma tissue after irradiation showed that proliferative potential of glioblastoma did not significantly change even after 60 Gy of irradiation. After conformal irradiation therapy up to 90 Gy,[25] the glioblasotma still retain proliferative potential in the area received 70 or 80 Gy of irradiation. Furthermore it was observed that damage to the glioblastoma is rather via vascular damage than direct effect to the tumor cells to show that glioma cells are really radioresistant.[13] Thus it should be noted that radiation therapy to glioma produced still unsatisfactory results and major advancement should be done to concur these barrier.

Drug Resistance

Chemotherapy of glioma has been known to have many problems also. However recent advancements highlighted chemotherapy of glioma again. Many studies since Cairncross et al,[7] showed that oligodendroglial tumors are chemosensitive to nitrosourea-vincristine-procarbazine combination chemotherapy.[20] Furthermore, this chemosensitivity has been reported to be related to some genetic changes.[8]

Temozolomide is an another recent topic in the chemotherapy of glioma. Many studies showes that this novel drug has activity against gliomas as well as metastatic brain tumor.[1] For recurrent anaplastic astrocytoma and anaplastic oligoastrocytoma, 45% recurrence-free survival for 6 months have been reported. Radiological study showed 35% response (CR and PR) rate and 26% stable disease.[30] Even in recurrent glioblastoma, 18% of the patients showed 6-months recurrence free period.[3]

Irrespective of these advances in glioma chemotherapy, brain tumors are still difficult target to treat with chemotherapy. The presence of of blood brain barrier (BBB) in the normal tissue is one of the reasons for the difficulty. The center of brain tumors usually lacks BBB, however area of tumor infiltration seems to have intact BBB. Brain tumor model in animals showed that in small tumor of less than 2 mm in diameter[28] or 0.2 mm^2 in area,[31] the BBB is preserved. These data suggest that BBB is intact in small tumors or area of infiltration thus chemotherapeutic agents would not be delivered to tumor cells in these lesions. Success of Temozolomide seems to be, at least partly, due to permeability of this drug through BBB.

Invasion

Invasiveness or infiltration of glioma is one of the major reasons of difficulty in the treatment of glioma. If gliomas were not invasive, the tumors can be cured, of course, by surgery alone, which is not the case.

In malignant glioma, especially in glioblastoma, tumor cells infiltrate far beyond the main tumor mass. The infiltrative tumor cells can be found as far as 3 cm away from the border of the neuroradiological image.[5,6] Before reviewing this invasiveness, general aspects of cancer cell invasion will be discussed.

Invasion of cancer cell is one of the most significant features of malignant tumor together with capability of distant metastasis. In fact, invasion and metastasis are so to say "two sides of the same coin". To establish metastatic foci

cancer cells must proceed sequential multiple steps and at each step invasion mechanisms or part of them work. Initially to create primary tumor mass, tumor cells needs blood supply. Angiogenic process takes place at this point. To leave the primary tumor, the tumor cells must get into the blood or lymphatic stream. To get into the blood or lymphatic vessel, the tumor cells have to degradate basement membrane of vessels, move (motility) and intravasate into vessels. Once get into the blood or lymphatic vessels, the tumor cells should escape from immune system to reach the target organ. At the target organ, the tumor cells have to attach to the endothelium, migrate between the endothelial cells, degradate the basement membrane again and lyse the local extracellar matrix. The tumor cells, then, have to proliferate in the target organ adjusting themselves to the local microenvironment. Interestingly, these are not random processes but certain tumor cells have a specific affinity to certain target organ ("seed and soil" phenomenon).[27] To complete metastatic process, the tumor cells have to have many features, i.e. high motility, high expression of degradating enzymes, high affinity to endothelial cells, higher expression of growth factor receptor which is suitable for the target organ and so on. That means the tumor cells which finally established metastasis were cells with multiple aptitude. Fidler, who is the authority of metastasis research mentioned that "Metastatic tumor cells are champion of decathlon". The word is an apt remark of multiple potential of metastatic cells.

As described above, invasion is one of the most remarkable features of malignant tumor cells. Many techniques *in vitro* and *in vivo* are employed to investigate metastatic phenotype of malignant tumor cells. *In vitro* research includes assay for protein, enzyme expression, and mRNA. *In vitro* experiments using cells to assess their invasiveness of many substrates including proteins consisting basement membrane or intracellular molecules.[2] Motility assay are also employed. *In vitro* experiments to see the interaction between the tumor cells and tissue or *in vivo* experiments to assess tumor host interaction are also important.

These methods were applied in the malignant brain tumor research also and with these many molecules have been reported to be involved in the pathophysiology of invasion of brain cancer. As for extracellular matrix component of brain, where the tumor cells to invade, laminin, collagen IV, tenascin, hyaluronic acid and brain enriched hyaluronan binding (BEHAB)/brevican have been in the list.[19,26,14] Heparan sulfate proteoglycan, collagen I, fibronectin, vitronectin and entactin are found in relation to basement membrane of blood vessels.[14,19,9] Another molecules, which mainly produced by tumor cells and related to tumor cell-matrix adhesion are integrins and hyaluronate receptor CD44.[4] Cadherins, selectins, neural cell adhesion molecule (NCAM), intercellular cell adhision molecule (ICAM) and vascular cell adhesion molecule (VCAM) have also been reported to be related to brain tumor invasion.[14,15] Another type of molecules which play major roles in degradating surrounding substrates are matrix metalloproteases (MMP) including MMP2 and MMP9.[24,21] However role of these MMPs are still controversial in some reports.

Balance between MMP and tissue inhibitor of metalloproteinase (TIMP) was also mentioned to be involved in tumor invasion.[10] Other degradating enzyme, urokinase-type plasminogen activator (uPA) and its receprot (uPAR) might be important.[22]

We have been investigating the role of lysophospholipase D (Lyso PLD)/autotaxin in glioma invasion. This molecule also seems to play some role in glioma invasiveness.

Glioma invasion is a complicated process but without overcoming this, cure of glioma would not be achieved.

Although many factors seem to be related to glioma invasion, further investigation is needed to integrate these findings.

In conclusion, many biological factors are related to malignant behavior of glioma as described here, including tumor cell genetics, proliferation, radiation- and chemosensitivity and invasive nature. Understanding of these factors will lead to better treatment and cure of this devastating disease.

REFERENCES

1) Abrey LE, Christodoulou C. *Temozolomide for treating brain metastases. Semin Oncol 28 : 34-42, 2001*
2) Albini A, Iwamoto Y, Kleinman HK, *et al. A rapic in vitro assay for quantitating the invasive potential of tumor cells. Cancer Res 47 : 3239-3245, 1987*
3) Brada M, Hoang-Xuan K, Rampling R, *et al. Multicenter phase II trial of temozolomide in patients with glioblastoma multiforme at first relapse. Ann Oncol 12 : 259-266, 2001*
4) Breyer R, Hussein S, Radu DL, *et al. Disruption of intracerebral progression of C6 rat glioblastoma by in vivo treatment with anti-CD44 monoclonal antibody. J Neurosurg 92 : 140-149, 2000*
5) Burger PC. *Pathologic anatomy and CT correlations in the glioblastoma multiforme. Appl Neurophysiol 46 : 180-187, 1983*
6) Burger PC, Dubois PJ, Schold SC, Jr., *et al. Computerized tomographic and pathologic studies of the untreated, quiescent, and recurrent glioblastoma multiforme. J Neurosurg 58 : 159-169, 1983*
7) Cairncross JG, Macdonald DR. *Oligodendroglioma : a new chemosensitive tumor. J Clin Oncol 8 : 2090-2091, 1990*
8) Cairncross JG, Ueki K, Zlatescu MC, *et al. Specific genetic predictors of chemotherapeutic response and survival in patients with anaplastic oligodendrogliomas. J Natl Cancer Inst 90 : 1473-1479, 1998*
9) Enam SA, Rosenblum ML, Edvardsen K. *Role of extracellular matrix in tumor invasion : migration of glioma cells along fibronectin-positive mesenchymal cell processes. Neurosurgery 42 : 599-607 ; discussion 607-598, 1998*
10) Fillmore HL, VanMeter TE, Broaddus WC. *Membrane-type matrix metalloproteinases (MT-MMPs) : expression and function during glioma invasion. J Neurooncol 53 : 187-202, 2001*
11) Fujimaki T. *Ki-67 antigen staining with MIB-1 monoclonal in brain tumors (review in Japanese). Byori to Rinsho 18 : 1032-1037, 2000*
12) Fujimaki T, Matsutani M, Nakamura O, *et al. Correlation between bromodeoxyuridine-labeling indices and patient prognosis in cerebral astrocytic tumors of adults. Cancer 67 : 1629-1634, 1991*
13) Fujimaki T, Matsutani M, Takakura K. *Analysis of BUdR (Bromodeoxyuridine) labeling indices of cerebral glioblastoma after radiation therapy. J Jpn Soc Ther Radiol Oncol 2, 1990*
14) Giese A, Laube B, Zapf S, *et al. Glioma cell adhesion and migration on human brain sections. Anticancer Res 18 : 2435-2447, 1998*
15) Goldbrunner RH, Bernstein JJ, Tonn JC. *Cell-extracellular matrix interaction in glioma invasion. Acta Neurochir (Wien) 141 : 295-305 ; discussion 304-295, 1999*
16) Hoshino T, Ahn D, Prados MD, *et al. Prognostic significance of the proliferative potential of intracranial gliomas measured by bromodeoxyuridine labeling. Int J Cancer 53 : 550-555, 1993*
17) Hoshino T, Barker M, Wilson CB, *et al. Cell kinetics of human gliomas. J Neurosurg 37 : 15-26, 1972*
18) Hoshino T, Nagashima T, Murovic J, *et al. Cell kinetic studies of in situ human brain tumors with bromodeoxyuridine. Cytometry 6 : 627-632, 1985*
19) Mahesparan R, Read TA, Lund-Johansen M, *et al. Expression of extracellular matrix components in a highly infiltrative in vivo glioma model. Acta Neuropathol (Berl) 105 : 49-57, 2003*
20) Mason WP, Krol GS, DeAngelis LM. *Low-grade oligodendroglioma responds to chemotherapy. Neurology 46 : 203-207, 1996*
21) Mercapide J, Lopez De Cicco R, Castresana JS, *et al. Stromelysin-1/matrix metalloproteinase-3 (MMP-3) expression accounts for invasive properties of human astrocytoma cell lines. Int J Cancer 106 : 676-682, 2003*
22) Mohanam S, Chintala SK, Go Y, *et al. In vitro inhibition of human glioblastoma cell line invasiveness by antisense uPA receptor. Oncogene 14 : 1351-1359, 1997*
23) Nagashima T, DeArmond SJ, Murovic J, *et al. Immunocytochemical demonstration of S-phase cells by anti-bromodeoxyuridine monoclonal antibody in human brain tumor tissues. Acta Neuropathol (Berl) 67 : 155-159, 1984*
24) Nakada M, Okada Y, Yamashita J. *The role of matrix metalloproteinases in glioma invasion. Front Biosci 8 : e261-269, 2003*
25) Nakagawa K, Aoki Y, Fujimaki T, *et al. High-dose conformal radiotherapy influenced the pattern of failure but did not improve survival in glioblastoma multiforme. Int J Radiat Oncol Biol Phys 40 : 1141-1149, 1998*
26) Nutt CL, Matthews RT, Hockfield S. *Glial tumor invasion : a role for the upregulation and cleavage of BEHAB/brevican. Neuroscientist 7 : 113-122, 2001*
27) Paget S. *The distribution of secondary growths in cancer of the breast. Lancet 1 : 571-573, 1889*
28) Yamada K, Ushio Y, Hayakawa T, *et al. Quantitative autoradiographic measurements of blood-brain barrier permeability in the rat glioma model. J Neurosurg 57 : 394-398, 1982*
29) Yoshii Y, Maki Y, Tsuboi K, *et al. Estimation of growth fraction with bromodeoxyuridine in human central nervous system tumors. J Neurosurg 65 : 659-663, 1986*
30) Yung WK, Prados MD, Yaya-Tur R, *et al. Multicenter phase II trial of temozolomide in patients with anaplastic astrocytoma or anaplastic oligoastrocytoma at first relapse. Temodal Brain Tumor Group. J Clin Oncol 17 : 2762-2771, 1999*
31) Zhang RD, Price JE, Fujimaki T, *et al. Differential permeability of the blood-brain barrier in experimental brain metastases produced by human neoplasms implanted into nude mice. Am J Pathol 141 : 1115-1124, 1992*

Technical Report

Intraoperative Tumor Segmentation and Volume Measurement in MRI-Guided Glioma Surgery for Tumor Resection Rate Control[1]

Nobuhiko Hata, PhD, Yoshihiro Muragaki, MD, PhD, Takashi Inomata, BS, Takashi Maruyama, MD, PhD, Hiroshi Iseki, MD, PhD, Tomokatsu Hori, MD, PhD, Takeyoshi Dohi, MD, PhD

Rationale and Objectives. Gross-total surgery under intraoperative magnetic resonance imaging (MRI) is a promising method of glioma removal. The purpose of this article is intraoperative measurement of resected tumor volume in MRI-guided glioma surgery using semiautomatic image segmentation to unbiased resection rate control.

Materials and Methods. A newly developed software program based on a fuzzy connectedness (FC) segmentation algorithm was used to achieve fast and semiautomatic tumor segmentation and tumor volume measurement. The program was validated by retrospective study of eight glioma cases and then applied to seven glioma cases. All clinical cases underwent actual MRI-guided surgery using 0.3-T open magnets.

Results. The volume of the tumor before resection ranged from 10.1 to 206.7 mL. A comparison of the results of manual segmentation with those of the semiautomatic FC-based segmentation gave an average dice similarity coefficient of 0.80 and an average match of 76%. Volume measurement combined with a developed software program enabled quantitative monitoring of tumor removal, which was critical in the near-total resection of glioma in MRI-guided surgery.

Conclusion. The FC-based tumor segmentation method can be used for intraoperative tumor segmentation and volume measurement in MRI-guided glioma surgery using 0.3-T open magnets. This method is useful for objective resection rate monitoring, which may ultimately minimize the amount of residual tumor in glioma surgery.

Key Words. MRI-guided surgery; brain tumor; segmentation; volume measurement.

The recurrence of glioma can be minimized by total or near-total surgical resection (1,2). Recognizing the importance of total resection of glioma, researchers have been trying to use intraoperative imaging to monitor the extent of tumor resection and ultimately increase the tumor resection rate in neurosurgery. The use of intraoperative imaging enables clear definition of the tumor boundary and observation of the extent of tumor removal during surgery. This real-time intraoperative information is critical to decision-making in tumor resection, which otherwise has to rely on preoperative x-ray computed tomography or magnetic resonance imaging (MRI) scans that do not reflect the current state of the cured lesions.

Intraoperative ultrasound is a widely spread and useful imaging modality for tumor craniotomy. Several studies

Acad Radiol 2005; 12:116–122

[1] From the Graduate School of Information Science and Technology, The University of Tokyo (N.H., T.I., T.D.), Institute of Advanced Biomedical Engineering & Science (Y.M., H.I.) and Department of Neurosurgery (T.M., T.H.), Tokyo Women's Medical University. Received August 4, 2004; revised October 20, 2004; accepted November 2, 2004. Grant-in-aid for scientific research (A-14702070) from the Ministry of Education, Culture, Sports, Science and Technology of Japan; Industrial Technology Research Grant Program in 2003 (A45003a and A47051a) from The New Energy and Industrial Technology Development Organization of Japan. **Address correspondence to** N.H. e-mail: noby@atre.t.u-tokyo.ac.jp

doi:10.1016/j.acra.2004.11.009

have investigated the effectiveness of intraoperative ultrasound in neurosurgical guidance (3,4). Hammoud and colleagues reported that intraoperative ultrasound facilitated the localization of metastases; however, in their study, the tumor was difficult to define with presurgical radiation therapy in 13 of 34 glioma cases (3). Chacko and colleagues obtained similar results (4) and found that the tumor was poorly defined in low-grade glioma cases. It should also be noted that although the use of three-dimensional (3D) ultrasound has become virtually mandatory in the volumetric observation of tumor removal, its clinical application is still in development (5–7). Mobile computed tomography with its intraoperative imaging capability is another option for guided tumor removal; however, it has not enjoyed widespread application because of the problem of patient and physician exposure to radiation (8).

Gross-total surgery under intraoperative MRI is a promising method of glioma removal. Following the seminal work of Black and colleagues to use open-configuration MRI for guiding craniotomy (9), Schneider and coworkers investigated the effectiveness of MRI-guidance for gross-total resection of glioma and reported an successful average tumor removal rate of 95.7% (10). In their study, total resection of the tumor was possible in 6 of the 12 cases. However, they also warned that the amount of residual tumor could be higher (5.5–15.5%) when the tumor is located close to eloquent areas. In all cases they investigated, the measurement of the tumor volume was an important tool for quantifying the amount of tumor resection, yet no description was given to clarify whether their measurement tool was feasible for intraoperative use (10).

The aim of this study was to develop a system of image processing tools for segmenting intraoperative volumetric images and measure the tumor volume during MRI-guided glioma surgery. Such tools can potentially enhance the location of residual tumor in MRI, facilitate tumor resection, and provide objective estimation of the extent of resection for more precise surgical control. The proposed method is based on a combination of algorithms that enable unbiased, accurate, and reliable measurement of tumor volume in intraoperative MRI. This method also satisfies the time requirements for intraoperative use. The accuracy of the proposed method of image segmentation was evaluated and compared with that of manual segmentation performed by an expert surgeon. The clinical usability of the method was assessed in five intraoperative applications.

Table 1
Patient Data

Case no.	Age	Sex	Grade	Lesion	Eloquent
1	66	F	1	Rt F	V p
2	33	F	3	Lt F	Broca
3	34	F	2	Rt F	CorpusCal
4	32	F	2	Rt T	V p
5	32	F	3	Rt P	CST p
6	48	F	2	RT F	—
7	37	M	3	Lt P	Sensory area
8	34	M	3	Rt F	—
9	55	F	3	Rt T	—
10	16	M	2	Lt T	Memory
11	34	F	3	Lt F	Speech (Broca)
12	39	F	2	Lt Insula	Speech (Broca)
Total/Average	38	F 9; M 3			

F, female; M, male; Rt, right; Lt, left; F, frontal; T, temporal lobe; P, parietal lobe; V, visual; p, pathway; CorpusCal, corpus callosum; CST, cortico-spinal tract.

MATERIALS AND METHODS

Patient Selection

Table 1 summarizes the list of cases discussed in this study. Twelve patients (nine women, three men; mean age 38 years) were diagnosed with glioma by using preoperative 1.5-T MRI. The following histologic diagnoses were obtained using the World Health Organization classification: one Grade 1, five Grade 2, and six Grade 3.

The internal review board of the hospital approved the intraoperative MRI-guided surgery and subsequent analysis by image processing, as well as the procedure for obtaining patient consent. The nature of the procedure was discussed with the patients, and informed consent was obtained following the internal review board guidelines.

Imaging Sequence

All patients underwent MRI-guided craniotomy in a 0.3-T open MRI scanner (AIRIS II TM, Hitachi Medical Co., Tokyo, Japan). The scanner provides intraoperative MRIs in the bore and makes it possible to slide the operative bed into an off-five Gauss-line area where the surgery is performed. Images were taken three times during the surgery: before the resection of the tumor (after craniotomy and dura opening); in the middle of the surgery when the majority of the tumor was thought to have been removed; and before dura closure after the resection of the tumor. Stereotactic navigation based on most recent